

Superparamagnetic behavior in ultrathin CoNi layers of electrodeposited CoNi/Cu multilayer nanowires

X.-T. Tang^{a)} and G.-C. Wang

Department of Physics, Applied Physics and Astronomy, Rensselaer Polytechnic Institute, Troy, New York 12180-3590

M. Shima

Department of Materials Science and Engineering, Rensselaer Polytechnic Institute, Troy, New York 12180-3590

(Received 15 January 2006; accepted 7 March 2006; published online 28 June 2006)

We present evidence that in a very thin regime the magnetic layers become discrete islands and superparamagnetic in multilayered CoNi(1–17 nm)/Cu(4.2 nm) nanowires grown by pulsed electrodeposition using a hole pattern of anodized alumina templates. Magnetic hysteresis loops measured at room temperature using a vibrating sample magnetometer show that superparamagnetism appears at $t(\text{CoNi}) < 1.7$ nm, due to a volumetric reduction of the CoNi layers that may result in discontinuity of the layer or formation of islands. The magnetic hysteresis loops for the superparamagnetic nanowires can be represented by the Langevin function. The temperature dependence of coercivity data obtained for the superparamagnetic nanowires using a superconducting quantum interference device indicates that the magnetization reversal can be consistently explained by the Stoner-Walferth model for coherent rotation. The volumetric reduction accounted for the observed superparamagnetism is probably due to an electrochemical exchange reaction between CoNi and Cu species at the interface during each Cu deposition cycle. The exchange reaction may cause partial dissolution of the CoNi layers at the interface which is eventually stabilized by cementation with Cu. The effects of the nucleation and growth process on the formation of superparamagnetic islands are also discussed. © 2006 American Institute of Physics. [DOI: 10.1063/1.2206854]

I. INTRODUCTION

Multilayer films consisting of alternating magnetic and nonmagnetic layers have attracted much attention since the discovery of giant magnetoresistance (GMR) effect.¹ When the thickness of each magnetic layer is reasonably large, the net magnetic moment of the layers can be thermally stable at ambient temperature often to give a sizable coercivity. When the magnetic layers become thinner, the volumetric magnetic energy may become small such that a superparamagnetic behavior may appear in the multilayers. In general, superparamagnetism is indicated by a hysteresis loop with reduced low-field susceptibility and virtually zero coercivity due to volumetric reduction of the magnetic layers. The superparamagnetic particles tend to randomly orient their magnetic moments due to thermal fluctuation. Néel explained that the thermal stability of magnetization in fine magnetic particles can be assessed by comparing the anisotropy energy KV (K : anisotropy constant; V : volume of a magnetic segment) and the thermal energy $k_B T$ (k_B : Boltzmann constant; T : temperature). When KV is decreased to a range comparable to or even smaller than $k_B T$, the particles become thermally unstable and superparamagnetism appears. In the case of multilayers, a superparamagnetic behavior can be observed when the dimensionality of the magnetic layers is reduced, which may cause a discontinuity of the layers if the layers are not

perfectly flat. Superparamagnetism has been observed in a variety of multilayer thin-film systems, such as Co/Au,^{2,3} Co/Cu,^{4,5} Ni/Cu,⁶ CoNi/Cu,⁷ and Fe/Tb⁸ through their magnetization and magnetoresistance measurements.

Previously reported superparamagnetism in multilayers was mostly studied using samples of a planar thin film that has a two-dimensional layered structure. The confined size in the lateral dimension of multilayered nanowires may exhibit a different magnetic behavior. The magnetic properties of multilayered nanowires, such as GMR, magnetization reversal mechanism, and superparamagnetism, can be controlled by varying their diameter and their magnetic or nonmagnetic layer thickness. It has been shown that multilayered nanowires can be grown into a hole pattern of a nanoporous template by a single-bath electrodeposition method.^{9–11} Among various electrodeposited magnetic multilayer systems, CoNi/Cu is of particular interest because of its relatively large GMR effect (55% at room temperature) and ease of layer thickness control owing to the small electrochemical dissolution of the magnetic layers at the copper deposition potential.^{12,13}

The goal of the present paper is to systematically study the magnetic properties of multilayered CoNi/Cu nanowires with particular focus on the CoNi layer thickness $t(\text{CoNi})$ dependent magnetic behavior in the small $t(\text{CoNi})$ regime. We varied $t(\text{CoNi})$ from 1 to 17 nm while keeping the Cu layer thickness constant at $t(\text{Cu})=4.2$ nm. We observed a superparamagnetic behavior in the very small $t(\text{CoNi})$ re-

^{a)}Electronic mail: tangx@rpi.edu

gime using a vibrating sample magnetometer (VSM) and a superconducting quantum interference device (SQUID) magnetometer. The average size of the superparamagnetic islands for each nanowire sample was estimated using the Langevin function fitted to the room-temperature hysteresis loops and the blocking temperature data obtained from low-temperature magnetization measurements. We will discuss the correlations of the roughness of the layers with their nucleation and growth process during the electrodeposition and the effects of anodic dissolution of CoNi during the subsequent Cu layer growth on the magnetic behavior and superparamagnetism. This report systematically investigates the magnetic layer thickness dependence of superparamagnetism in multilayered nanowire systems.

II. EXPERIMENT

The CoNi/Cu multilayer nanowires were grown into a hole pattern of commercial anodized alumina templates (Whatman, Anodisc) of 60 μm in thickness and 20 nm in nominal pore size. According to the information supplied by the vendor, each 60- μm -long pore consists of two portions: one end has pores of 20 nm in diameter and 1–2 μm in length and the other end with pores of 250 nm in diameter and 58–59 μm in length. Prior to electrodeposition of CoNi/Cu nanowires, an 80-nm-thick Au film was coated onto the 20 nm pore side of the template using thermal evaporation. The electrodeposition was carried out using a classical three-electrode system including a Ag/AgCl reference electrode and a platinum counter electrode. An electrolytic solution containing 2.3M $\text{Ni}(\text{SO}_3\text{NH}_2)_2$, 0.4M CoSO_4 , 0.025M CuSO_4 , and 0.5M H_3BO_3 was maintained at the pH of 2.2 at room temperature during the electrodeposition. All the electrodes were positioned vertically. A pulsed electrodeposition technique was used by periodically switching the deposition potential between -0.2 V for Cu and -1.0 V for CoNi layer depositions. The detailed description for the method of multilayer electrodeposition can be also found elsewhere.^{10,14,15} The thickness of each layer is controlled by optimizing the pulse duration and the cumulative charge transferred during the pulse. The actual layer thicknesses for magnetic and nonmagnetic layers were determined by visually examining the multilayer structure using scanning electron microscopy (SEM). In order to clearly identify the CoNi and Cu layers in the SEM images and to estimate the growth rate, multilayer nanowires with the thicknesses for both CoNi and Cu layers larger than those used for magnetic characterization were specially prepared and utilized. In order to remove the nanowires from the template, the alumina template was dissolved away by submerging the sample in a NaOH solution. The average growth rates for CoNi and Cu layers were approximately 17 ± 2 and 0.21 ± 0.04 nm/s, respectively. These values were estimated from the actual layer thickness, obtained from the SEM images, divided by the pulse durations. It should be noted that the growth rate for multilayer samples might vary with changing the thickness of the layers since the cementation effect is expected to be more significant for films with a thinner layer thickness. The overall chemical compositions of CoNi/Cu samples were

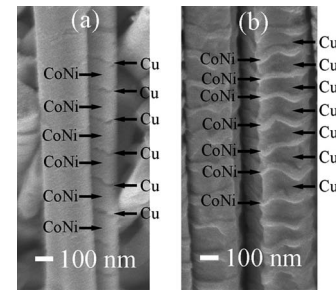


FIG. 1. SEM images for multilayered CoNi/Cu nanowires with the layer thicknesses of (a) $t(\text{CoNi})=155 \pm 9$ nm and $t(\text{Cu})=18 \pm 3$ nm and of (b) $t(\text{CoNi})=33 \pm 9$ nm and $t(\text{Cu})=95 \pm 26$ nm.

measured using energy dispersive spectroscopy (EDS) available in a SEM. The number of cycles was varied with samples in order to keep the total length of the nanowires constant at about 20 μm . Magnetic characterization of the nanowire samples was carried out before removing the alumina template used for the growth. The magnetic hysteresis loops were measured at room temperature using VSM, with magnetic fields applied either perpendicular or parallel to the wire axis. The magnetization was measured at temperatures from 5 to 300 K using SQUID.

III. RESULTS AND DISCUSSIONS

The structure of the multilayer nanowires was first examined using SEM (see Fig. 1). The image for CoNi/Cu nanowires shown in Fig. 1(a) demonstrates that the wires indeed have a multilayered structure consisting of periodically alternating CoNi and Cu layers with a larger thickness value of $t(\text{CoNi})=155 \pm 9$ nm and a smaller value of $t(\text{Cu})=18 \pm 3$ nm, respectively. In contrast, the multilayer nanowires shown in Fig. 1(b) have a smaller thickness value $t(\text{CoNi})=33 \pm 9$ nm for CoNi and a larger value $t(\text{Cu})=95 \pm 26$ nm for Cu. The images obtained from these samples also show that the individual layers are not perfectly flat since a waviness of the interfaces is readily observed in most of the layers. It is inferred from this observation that the interfacial roughness tends to increase with decreasing layer thickness and the layers may eventually become discontinuous below some critical layer thickness.

Figure 2 shows room-temperature magnetic hysteresis loops measured for CoNi/Cu nanowires with various CoNi layer thicknesses in magnetic fields applied perpendicular to the wire axis. When $t(\text{CoNi}) \geq 6.8$ nm [the loop for $t(\text{CoNi})=6.8$ nm is shown in Fig. 2(a)], the nanowire samples have relatively large coercivities indicating that the magnetic behavior of the nanowires is ferromagnetic. The coercivity H_C decreases when $t(\text{CoNi}) \leq 6.8$ nm [see the loops for $t(\text{CoNi})=3.5$ nm in Fig. 2(b) and $t(\text{CoNi})=2.0$ nm in Fig. 2(c)]. When $t(\text{CoNi}) \leq 1.7$ nm [see the loop for $t(\text{CoNi})=1.0$ nm in Fig. 2(d)], the hysteresis loop exhibits typical characteristics of superparamagnetism: gradual increase of the magnetization at low fields and vanishing coercivity. The observed change in the hysteresis loops with decreasing $t(\text{CoNi})$ is clearly represented in the $t(\text{CoNi})$ dependence of H_C in Fig. 3. As $t(\text{CoNi})$ decreases from 17 to 6.8 nm, the room-temperature coercivity increases

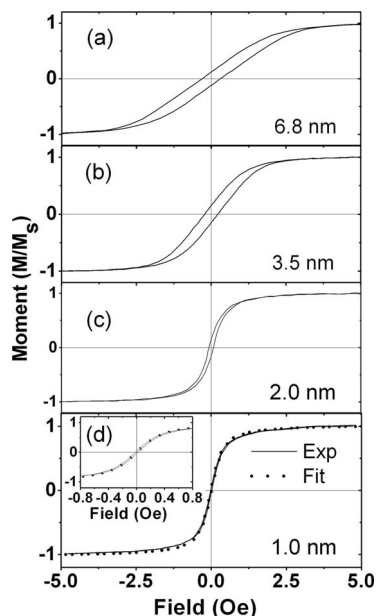


FIG. 2. Magnetic hysteresis loops measured at room temperature by VSM for CoNi/Cu nanowires with $t(\text{Cu})=4.2$ nm and various magnetic layer thicknesses: (a) $t(\text{CoNi})=6.8$ nm, (b) $t(\text{CoNi})=3.5$ nm, (c) $t(\text{CoNi})=2.0$ nm, and (d) $t(\text{CoNi})=1.0$ nm. The dotted line in (d) represents a loop fit using the Langevin function. The inset for (d) shows the same loop in the low field range of $(-0.8$ to 0.8 kOe).

from 268 to 305 Oe. The observed increase in H_C is similar to previously reported results showing that H_C increases with decreasing film thickness,¹⁶ where H_C linearly increases from 25 to 192 Oe as the thickness of the Co layers decreases from 200 to 2.5 nm. However, their results are different from our case for $t(\text{CoNi}) < 6.8$ nm. In our case H_C decreases rapidly to 8 Oe at $t(\text{CoNi})=1.7$ nm when $t(\text{CoNi})$ decreases from 6.8 to 1 nm.

The observed magnetic transition of the multilayer nanowires from the ferromagnetic to superparamagnetic states can be consistently explained in terms of the morphological change in the magnetic layers, namely, the continuity of the layers breaks down, and each layer rather consists of discrete segments with much smaller volume. The superparamagnetic state of a fine particle system can be realized when the particles are so small that their magnetic moments become thermally unstable at a given temperature. In order to thermally

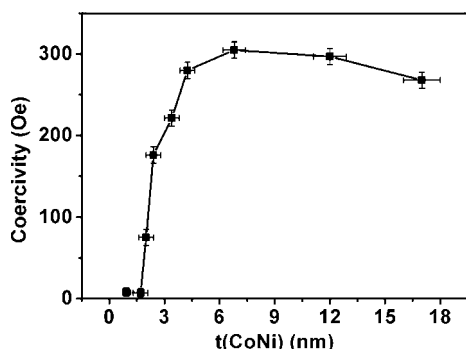


FIG. 3. Coercivities for CoNi/Cu nanowires with various CoNi layer thicknesses $t(\text{CoNi})$ measured at room temperature by VSM in magnetic fields applied perpendicular to the wire axis. The Cu layer thickness $t(\text{Cu})$ is fixed at 4.2 nm for all the samples.

change the magnetization direction of the particles from the easy axis to another, the particles need to gain thermal energy that is higher than the anisotropy energy KV , where K and V are the anisotropy constant and particle's volume, respectively. When V decreases at constant K , the anisotropy energy KV decreases and eventually becomes comparable or smaller than the thermal energy $25 k_B T$ at the blocking temperature T_B . When the magnetization is measured at temperatures greater than T_B , thermal fluctuations of the magnetic moments in the fine particles reduce the effective magnetization measured in a time scale of data acquisition, which gives a superparamagnetic hysteresis loop with vanishing coercivity.

The magnetization of a superparamagnetic fine particle can be expressed by the Langevin function,

$$M/M_s = \coth(\alpha) - 1/\alpha, \quad (1)$$

where $\alpha = \mu(H - H_{\text{eff}})/k_B T$ and H_{eff} is an effective magnetic field or demagnetizing field from the adjacent particles. The dotted line in Fig. 2(d) represents a least-square fit to the experimental data using the Langevin function, which gives a good agreement with the experimental values. The magnetic moment of a superparamagnetic particle in the system can be extracted from the Langevin parameter α . We found that the estimated volume of the superparamagnetic islands is significantly smaller than that for a single continuous CoNi layer, indicating that the CoNi layers are not actually continuous but consisting of discrete islands within the layers. The estimated room-temperature magnetic moment μ per island for the CoNi/Cu nanowires with $t(\text{CoNi})=1.0$ nm is $(2.9 \pm 0.5) \times 10^4 \mu_B$, where μ_B is the Bohr magneton. Similarly, the moment per island for $t(\text{CoNi})=1.7$ nm is $(3.4 \pm 0.8) \times 10^4 \mu_B$. The increase in the moment with increasing $t(\text{CoNi})$ may simply be due to the increased size of the superparamagnetic islands.

When $T < T_B$, the thermal energy $k_B T$ is not high enough to cause a thermal instability of the magnetic moment so the moment is stabilized along an easy axis, which represents a ferromagnetic state. Figure 4(a) shows the second quadrant of the hysteresis loops for $t(\text{CoNi})=1.0$ nm, measured at various temperatures in magnetic fields applied perpendicular to the wire axis after saturated at 10 kOe.

For ultrathin CoNi layers, each island may be in a single domain state as the total magnetic energy can be minimized. The magnetization reversal of a single domain magnet can be represented by the Stoner-Walferth model for coherent rotation or the curling mode. In the case of CoNi/Cu multilayer nanowires, we assume a magnetization reversal by coherent rotation, since the coherent rotation can minimize the exchange energy, which becomes the largest for very fine particles such as small islands in the CoNi layers. The temperature dependence of coercivity is then analytically expressed as

$$H_c = H_{c0} [1 - (T/T_B)^{1/2}], \quad (2)$$

where H_{c0} is the coercivity at 0 K. The temperature dependence of coercivity for the samples with $t(\text{CoNi})=1.7$ and 1.0 nm is shown in the curves in Fig. 4(b). The dotted lines represent the fit of data calculated from Eq. (2). The $T^{1/2}$

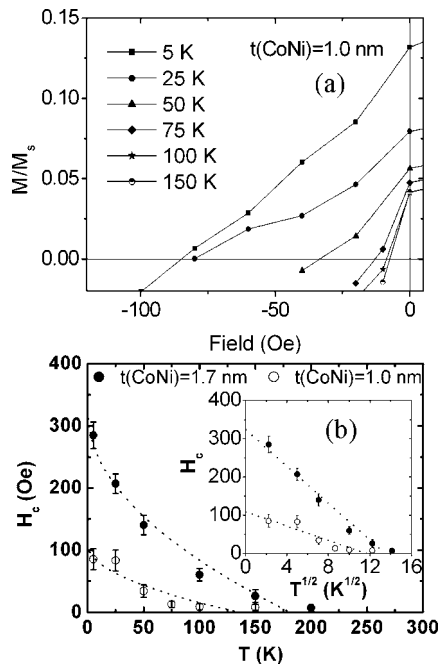


FIG. 4. Magnetization data for CoNi/Cu nanowires obtained by SQUID with magnetic fields applied perpendicular to the wire axis at various temperatures; (a) temperature variation of magnetic hysteresis loops for $t(\text{CoNi})=1.0$ nm (only those in the fields around the coercivities are shown) and (b) coercivities (H_c) plotted as a function of the temperature (T) for $t(\text{CoNi})=1.0$ nm and $t(\text{CoNi})=1.7$ nm. The inset for (b) represents the same coercivity data plotted as a function of $T^{1/2}$. The dotted lines are the fitted curves assuming a coherent rotation for the magnetization reversal.

dependence of coercivity shown in the inset of Fig. 4(b) shows that the experiment data agrees fairly well with the data calculated from Eq. (2). For example, T_B for the sample with $t(\text{CoNi})=1.7$ nm is around 181 K, while that for $t(\text{CoNi})=1.0$ nm is around 136 K [see their curves in Fig. 4(b)].

To assess the island size extracted from the room-temperature hysteresis loop for the sample with $t(\text{CoNi})=1.0$ nm, we estimated the volume of the individual islands from the blocking temperature. In the first approximation, it is reasonable to assume that the anisotropy energy of the CoNi layers in the nanowires is mainly contributed by the shape anisotropy. $K=2\pi M_s^2$ since the demagnetizing factor is 4π (cgs unit) in the direction perpendicular to the interfaces and nearly 0 in the direction parallel to the interfaces. The critical volume V_C for the superparamagnetism is $V_C=25kT_B/2\pi M_s^2$. For $t(\text{CoNi})=1.0$ nm, the saturation magnetization M_s is ~ 640 emu/cm³ which corresponds to an anisotropy constant $K=2.6 \times 10^6$ erg/cm³. The critical volume for $T_B=136$ K is 182 nm³.

If we assume that the thickness of the layers is uniform, the critical value for the magnetic layer thickness of nanowires with a diameter of 250 nm should be 3.7×10^{-3} nm, which is so small that the layers are likely to be discontinuous. An island with the volume of 182 nm³ would consist of approximately 1.65×10^4 atoms. For simplicity, assuming that the magnetic atoms carry the same magnetic moment as that for the bulk, that is, $1.7\mu_B$ for Co and $0.6\mu_B$ for Ni, then the average atomic moment for $\text{Co}_{55}\text{Ni}_{45}$ is $1.2\mu_B$ or the moment per island is $(2.0 \pm 0.7) \times 10^4 \mu_B$. Similarly, the mag-

TABLE I. Average magnetic moments of CoNi islands obtained from the fit of magnetization hysteresis loops using Eq. (1), and from the temperature dependence of coercivity using Eq. (2). The values for $t(\text{CoNi})$ represent the thicknesses of the CoNi layers in the multilayer nanowires with 4.2-nm-thick Cu layer.

$t(\text{CoNi})$ (nm)	$\mu(\times 10^4 \mu_B)$ [Eq. (1)]	$\mu(\times 10^4 \mu_B)$ [Eq. (2)]
1.0	2.9 ± 0.5	2.0 ± 0.7
1.7	3.4 ± 0.8	2.6 ± 0.8

netic moment per island for $t(\text{CoNi})=1.7$ nm is $(2.6 \pm 0.8) \times 10^4 \mu_B$ (see Table I). It should be noted that the estimated value is smaller than the previous obtained value using the Langevin function since the anisotropy constant used for the calculation may be overestimated because we consider only the shape anisotropy in this analysis. The actual anisotropy of the system may be contributed by different anisotropy terms such as shape, surface, stress, and magnetocrystalline anisotropies.

The formation of a superparamagnetic fine structure in the CoNi layers may be attributed to an exchange reaction, that is, an electrochemical stripping of CoNi at the interface during the electrodeposition of the subsequent Cu layer. Namely, a dissolution of previously deposited less noble CoNi atoms is involved simultaneously during the deposition of more noble Cu atoms.^{6,7} The growth front, which is electrochemically active, is likely to induce a local intermixing between the surface CoNi atoms and depositing Cu species, which may result in the formation of relatively ill-defined interfaces between layers. We speculate that such interfacial reactions occur inhomogeneously during the multilayer growth, which results in a formation of rough and wavy interfaces as well as a variation of the CoNi layer thickness observed in the SEM images. In the case of multilayer nanowires with very thin CoNi layers, a random dissolution of the magnetic layers can cause a lateral variation of the layer thickness and lead to a formation of the discontinuous layer structure in the CoNi layers. The discrete regions of the magnetic layers can exhibit a superparamagnetism due to their reduced dimensions. Indeed a superparamagnetic behavior in multilayer nanowire samples with $t(\text{CoNi}) < 1.7$ nm was observed. However, the discrete regions in the CoNi layers periodically embedded in the Cu matrix are expected to have a wide range of size distribution. In such a case, some regions with smaller dimensions may exhibit superparamagnetism, while others with larger dimensions show a ferromagnetic behavior when measured at a temperature near the blocking temperature.

It should be noted that the critical value of the magnetic layer thickness for the onset of superparamagnetism we observed is apparently larger than subnanometer-thick Co layer for Co/Cu multilayer thin films previously reported.^{3,4,17-19} In the case of CoNi/Cu nanowires, the maximum coercivity is obtained at $t(\text{CoNi})=6.8$ nm when $t(\text{CoNi})$ is varied, indicating that the CoNi layers begin to break into discontinuous regions at $t(\text{CoNi}) < 6.8$ nm. In the case of Co/Cu multilayer films made by electrodeposition, Voegeli *et al.* pointed out that 3 nm is the minimum layer thickness beyond which re-

producibile and reliable magnetic data can be obtained.²⁰ We speculate that there are at least three factors that can affect the thickness variation of the layers as observed in the SEM images.

First, stress can be exerted on the nanowires which are in contact with the sidewall of the pores in the rigid alumina template. A strain in the nanowires induced by the stress from the sidewall of the pores may also contribute to developing the waviness of the layers.

Second, the conducting coating surface which serves as a cathode for electrodeposition in the pores of the template may have some roughness that may induce the waviness in the layers grown onto the surface. In general, the nucleation and growth process during the deposition is sensitively influenced by various factors including the crystallographic orientation of the original surface, the surface energy, and the kinetic energy of the depositing species. If the surface contains some defects such as step edges and grain boundaries, nuclei are preferentially formed at such defect sites.²¹ Therefore, the quality of the conducting coating surface may critically govern the quality of the layers grown on it. Since the conducting coating surface is indeed relatively rough, a rms roughness of about 20 nm as inferred by atomic force microscopy, the multilayer nanowires grown on it may inherit such a roughness and develop some waviness in the layers.

Third, although the sidewall of the pores is electrically insulating, it is still possible that the surface of the wall serves as a nucleation site for depositing species. As described earlier, the Au conducting coating was evaporated on the backside of the template. It is possible that Au might also be coated on the sidewall of the pores at the edge or in the vicinity of the apertures before completely covering the pores.^{22,23} In the beginning of the CoNi/Cu nanowire electrodeposition, some of the depositing species might grow on the Au-coated part of the sidewalls, which contributed to the roughness of the layers.

IV. CONCLUSIONS

We have observed a superparamagnetic behavior in ultrathin CoNi layer regime of electrodeposited CoNi/Cu multilayer nanowires. With decreasing the magnetic layer thickness to less than 6.8 nm, a superparamagnetic behavior begins to appear at room temperature due to the reduced volume of the individual magnetic layers. In this regime, the magnetic layers are so thin that some of the layers become discontinuous and superparamagnetic, while others are still continuous and ferromagnetic. With further decreasing the magnetic layer thickness to 1.7 nm, most of the magnetic layers become discontinuous and superparamagnetic. The magnetization of the superparamagnetic nanowires above their blocking temperatures can be described using the Langevin function. The temperature dependence of the coercivity approximately follows the Stoner-Walferth model for coherent rotation. The transition of the magnetic behavior of CoNi/Cu nanowires from ferromagnetic to superparamag-

netic upon reducing the CoNi layer thickness may be related to the morphological change in the CoNi layers from continuous to discontinuous. The discontinuity in very thin magnetic layers is clued from the waviness and the thickness variation of the layers in the nanowires as observed by SEM.

The knowledge about the structure-magnetic property relations obtained in this study will be useful in understanding the magnetotransport properties such as GMR. To minimize the superparamagnetic effect, which is detrimental in data storage application, the layer and interface quality should be improved. To achieve this, work should be concentrated on minimizing the exchange reaction, obtaining a high quality conducting layer as a cathode electrode, and a better control of the nucleation and growth process.

ACKNOWLEDGMENTS

The work was supported by the seed grant of Rensselaer Polytechnic Institute and the National Science Foundation Award No. 05 06 738. We thank D.-X. Ye for taking the SEM images.

¹M. N. Baibich *et al.*, Phys. Rev. Lett. **61**, 2472 (1988).

²J. Xu, M. A. Howson, B. J. Hickey, D. Greig, P. Veillet, and E. Kolb, J. Magn. Magn. Mater. **156**, 379 (1996).

³J. Xu, M. A. Howson, B. J. Hickey, and D. Greig, Phys. Rev. B **55**, 416 (1997).

⁴M. Shima, L. Salamanca-Riba, R. D. McMichael, and T. P. Moffat, J. Electrochem. Soc. **149**, C439 (2002).

⁵I. Bakonyi, L. Péter, Z. Rolik, K. Kiss-Szabó, Z. Kupay, J. Tóth, L. F. Kiss, and J. Pádár, Phys. Rev. B **70**, 054427 (2004).

⁶I. Bakonyi, J. Tóth, L. Goualou, T. Becsei, E. Tóth-Kádár, W. Schwarzacher, and G. Nabiyouni, J. Electrochem. Soc. **149**, C195 (2002).

⁷G. Nabiyouni, W. Schwarzacher, Z. Rolik, and I. Bakonyi, J. Magn. Magn. Mater. **253**, 77 (2002).

⁸F. Yang, T. He, J. B. Chen, and F. Pana, J. Appl. Phys. **91**, 3114 (2002).

⁹L. Piraux, J. M. George, J. F. Despres, C. Leroy, E. Ferain, R. Legras, K. Ounadjela, and A. Fert, Appl. Phys. Lett. **65**, 2484 (1994).

¹⁰W. Schwarzacher and D. S. Lashmore, IEEE Trans. Magn. **32**, 3133 (1996).

¹¹A. Fert and L. Piraux, J. Magn. Magn. Mater. **200**, 338 (1999).

¹²W. Schwarzacher, K. Attenborough, A. Michel, G. Nabiyouni, and J. P. Meier, J. Magn. Magn. Mater. **165**, 23 (1997).

¹³P. R. Evans, G. Yi, and W. Schwarzacher, Appl. Phys. Lett. **76**, 481 (2000).

¹⁴M. Shima, L. Salamanca-Riba, T. P. Moffat, R. D. McMichael, and L. J. Swartzendruber, J. Appl. Phys. **84**, 1504 (1998).

¹⁵X.-T. Tang, G.-C. Wang, and M. Shima, J. Appl. Phys. **99**, 033906-1 (2006).

¹⁶M. Cerisier, K. Attenborough, J.-P. Celis, and C. Van Haesendonck, Appl. Surf. Sci. **166**, 154 (2000).

¹⁷F. Spizzo, E. Angeli, D. Bisero, P. Vavassori, and F. Ronconi, Appl. Phys. Lett. **79**, 3293 (2001).

¹⁸F. Spizzo, E. Angeli, D. Bisero, P. Vavassori, and F. Ronconi, J. Magn. Magn. Mater. **242**, 473 (2002).

¹⁹P. Vavassori, F. Spizzo, E. Angeli, D. Bisero, and F. Ronconi, J. Magn. Magn. Mater. **262**, 120 (2003).

²⁰B. Voegeli, A. Blondel, B. Doudin, and J.-Ph. Ansermet, J. Magn. Magn. Mater. **151**, 388 (1995).

²¹D. Bera, S. C. Kuiry, and S. Seal, JOM **56**, 49 (2004).

²²L. Wang, K. Yu-Zhang, A. Metrot, P. Bonhomme, and M. Troyon, Thin Solid Films **288**, 86 (1996).

²³S. Valizadeh, L. Hultman, J. M. George, and P. Leisner, Adv. Funct. Mater. **12**, 766 (2002).